Plasma Physics and Controlled Fusion, Vol. 29, No. 6, pp. 719 to 727, 1987
Printed in Great Britain.

0741-3335/87$3.00 + .00
IOP Publishing Ltd. and Pergamon Journals Ltd.

RESISTIVE BALLOONING MODES AND THE SECOND REGION OF STABILITY

A. SYKES, C. M. BISHOP and R. J. HASTIE
Culham Laboratory, Abingdon, Oxfordshire, OX14 3DB, U.K.
(EURATOM/UKAEA Fusion Association)

(*Received* 18 *October* 1986)

Abstract—Resistive ballooning modes are unstable in the first region of ideal ballooning stability. We show that in contrast the second region is largely stable to resistive ballooning modes.

1. INTRODUCTION

TOKAMAK equilibria which are stable to ideal MHD perturbations may be unstable to resistive modes (FURTH *et al.*, 1963). Of particular interest is the resistive ballooning mode which has been suggested by CHANCE *et al.* (1979) as a candidate to explain the energy confinement degradation seen in L-mode scaling. Since resistive modes have a much lower growth rate than ideal modes they need only be considered in plasmas which are ideally stable. At low values of the radial pressure gradient Tokamak equilibria are stable to localised ideal MHD ballooning modes; this is referred to as the first stable region. Higher pressure gradients destabilise the ideal ballooning mode, but at sufficiently large gradients the plasma is again ideally stable. This is known as the second region of stability. Figure 1 shows the well-known s-α diagram which illustrates the presence of two stable regions; this diagram is discussed again in Section 2.

Resistive ballooning modes have, in common with tearing modes, the property that their stability is determined by the asymptotic matching of ideal MHD solutions in an outer region to non-ideal solutions valid in the neighbourhood of the singular layers. Many physical effects come into play within the layers, but the influence of the ideal region, either stabilising or destabilising, is determined by one real quantity, Δ', which can be simply computed from the ideal ballooning equation. As in tearing mode theory, Δ' (the ratio of the large to the small solutions as the singularity is approached) is a measure of the energy available to drive the instability.

CONNOR *et al.* (1983) and DRAKE and ANTONSEN (1985) studied stability using single fluid resistive equations to describe the behaviour in the singular layer. For a fixed, finite value of the toroidal mode number n, it was found that instability occurred whenever Δ' exceeded some critical value Δ'_c. However, CONNOR *et al.* (1985) found, using the two-fluid equations, that resistive ballooning modes should be unstable whenever $\Delta' > 0$. CONNOR *et al.* (1983), DRAKE and ANTONSEN (1985) and CONNOR *et al.* (1985) all found that within the first region of ideal stability, $\Delta' > 0$; therefore in this region resistive ballooning modes are unstable.

In Section 2 we introduce the large aspect ratio model equilibrium which forms the basis of our investigations. Its resistive ballooning stability in the first region is examined in Section 3 and compared with other published results.

Stability in the second region is studied in Section 4. CORREA-RESTREPO (1985) showed that in certain situations the second region is unstable due to resistive interchange modes. We shall show more generally, however, that the second region is largely stable to both resistive ballooning and resistive interchange modes. Inclusion of the Shafranov shift effect, as described in Section 5, further enhances the stability.

Finally in Section 6 we discuss the relevance of the second region to fusion experiments and list some methods by which it may be accessed.

2. THE MODEL TOKAMAK EQUILIBRIUM

To investigate the stability of resistive ballooning modes we consider a large aspect ratio Tokamak equilibrium constructed in the neighbourhood of a circular flux surface on which the poloidal magnetic field is taken to be a constant. This is the s-α model of CONNOR *et al.* (1978). Stability properties are determined from the second order equation

$$\frac{\mathrm{d}}{\mathrm{d}\theta}\left\{[1 + (s(\theta - \theta_0) - \alpha \sin \theta)^2]\frac{\mathrm{d}F}{\mathrm{d}\theta}\right\} + \alpha\{\cos\theta + \sin\theta(s(\theta - \theta) - \alpha\sin\theta)\}F = 0 \quad (1)$$

where F is the plasma displacement and θ is the poloidal angle. As a result of the ballooning transformation (CONNOR *et al.*, 1979) the angle θ lies on $[-\infty, \infty]$. The parameters s and α describing the shear and the radial pressure gradient respectively are defined by

$$s = \frac{r}{q}\frac{\mathrm{d}q}{\mathrm{d}r} \quad (2)$$

$$\alpha = -\frac{2Rq^2}{B_0^{\,2}}\frac{\mathrm{d}p}{\mathrm{d}r} \quad (3)$$

where r and R are the minor and major radii, q is the safety factor, p is the plasma pressure, and B_0 is the toroidal magnetic field on axis.

Equation (1) describes plasma displacements in regions away from the reconnection surface. For large values of θ the solutions of equation (1) should be matched onto those from the resistive layer. Asymptotic behaviour of the solutions of equation (1) is given by

$$F(\theta) = af(\theta) + \frac{b}{s(\theta - \theta_0)}f(\theta) \quad (4)$$

where

$$f(\theta) = 1 + \frac{\alpha\sin\theta}{s(\theta - \theta_0)} + \frac{\alpha\cos\theta}{s^2(\theta - \theta_0)^2} - \frac{\alpha^2\sin^2\theta}{2s^2(\theta - \theta_0)^2} + 0((s\theta)^{-3}). \quad (5)$$

Instead of matching on to resistive solutions, we make use of the results of CONNOR *et al.* (1985) and determine the stability to resistive ballooning modes by constructing Δ' defined by

$$\Delta' = \frac{b}{sa}. \tag{6}$$

CONNOR *et al.* (1985) showed that these modes will be unstable if $\Delta' > 0$. To calculate Δ' from equation (1) first consider the case where the parameter $\theta_0 = 0$. The equation is then symmetric under $\theta \rightarrow -\theta$ and there are two classes of solution, one F_+ with the initial conditions $F(0) = 1, F'(0) = 0$ and the other F_- having $F(0) = 0$, $F'(0) = 1$. The first of these is the resistive ballooning mode while the second is the micro-tearing mode. The full solutions are then matched onto the asymptotic form (4) at some large value θ_{max}, to obtain values for the coefficients a and b. Δ' is then calculated from equation (6). If, however, $\theta_0 \neq 0$ then equation (1) must be solved on $[-\theta_{max}, \theta_{max}]$ and the full solution will be some mixture of the basic solutions F_+ and F_- (obtained now with $\theta_0 \neq 0$), subject to the constraint that $\Delta'(\theta_{max}) = \Delta'(-\theta_{max})$. (This follows from the symmetry of the resistive layer equations which are independent of θ_0.) Again there will be two solutions which can be identified as a resistive ballooning and a micro-tearing mode. The value of θ_0 is chosen so as to maximise the value of Δ'.

Since the asymptotic region corresponds to $s\theta \gg 1$ the calculation of the numerical solution out to the asymptotic region becomes increasingly difficult for small values of s. There are effectively two length scales in the problem, $\theta \sim 1$ on which equilibrium quantities vary, and $\theta \sim 1/s$ defining the asymptotic region. For $s \ll 1$ we can obtain averaged equations in which the short length scale is integrated out leaving much simpler equations on the long scale. This is done in detail in Appendix A. Evaluations of Δ' from the averaged equations are found to join on smoothly to those from the full equations at intermediate values of s.

3. RESISTIVE BALLOONING IN THE FIRST REGION

Ideal marginal stability boundaries correspond to solutions of equation (1) for which the coefficient a of the large solution vanishes. This defines an eigenvalue problem whose solutions are curves in the s-α plane along which $\Delta' = \infty$. This is shown in Fig. 1.

Evaluating Δ' in the first ideally stable region we find that $\Delta' > 0$. This is illustrated in Fig. 2 which shows Δ' plotted as a function of α for $s = 1$. Also plotted in Fig. 2 is the Δ' given by DRAKE and ANTONSEN (1985) who considered a model equilibrium valid in the neighbourhood of the axis with $\beta \sim \varepsilon^2$. There is complete agreement with the $\alpha \ll 1$ limit of our results while for larger values of α the results of DRAKE and ANTONSEN (1985) differ from those of the full high $\beta(\beta \sim \varepsilon)$ equations and fail completely to represent the approach to the ideal unstable region.

STRAUSS (1981) has also considered resistive ballooning stability for an equilibrium constructed around the axis. Averaged equations were obtained valid when $s \ll 1$. Results for Δ' in the first region given in STRAUSS (1985) are in complete agreement with the $s \ll 1$ limit of our results.

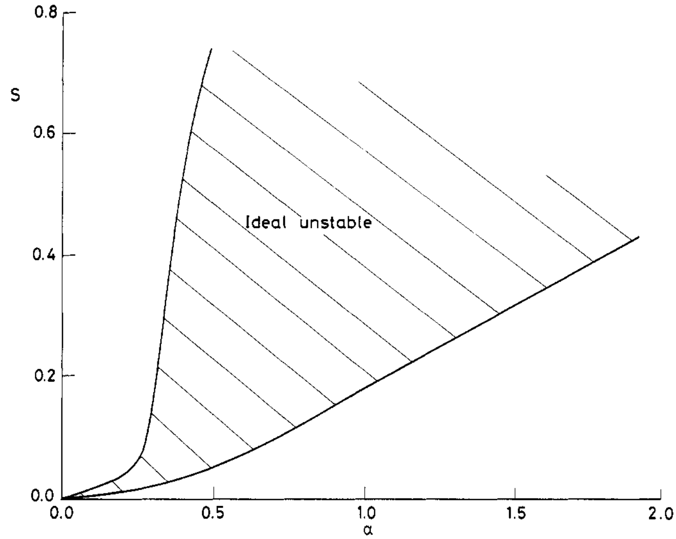

FIG. 1.—The $s - \alpha$ plane showing the ideal marginal stability curves and the first and second stable regions.

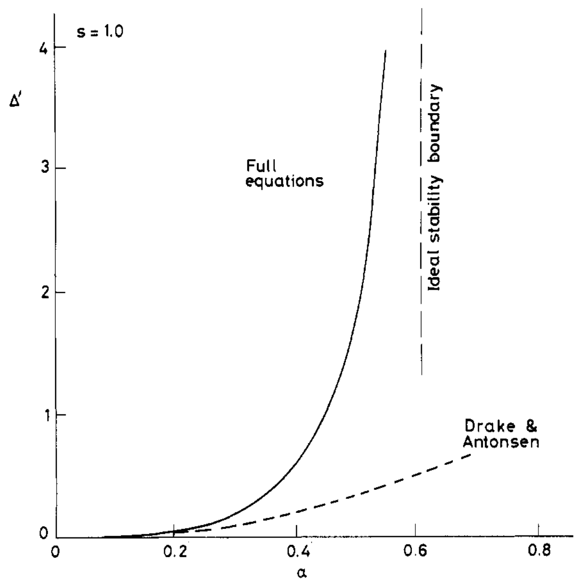

FIG. 2.—Plot of Δ' versus α for $s = 1$ obtained from the solution of equation (1). The broken curve shows the corresponding Δ' calculated by DRAKE and ANTONSEN (1985) valid for $\alpha \ll 1$.

Resistive ballooning has been studied by CORREA-RESTREPO (1985) again for equilibria valid near the axis. An analytic expression for Δ' was obtained which gives $\Delta' > 0$ throughout the first region.

4. RESISTIVE BALLOONING IN THE SECOND REGION

Evaluation of Δ' in the second stable region using equation (1) shows that $\Delta' < 0$ throughout most of this region. This is shown on an s-α diagram in Fig. 3. For pressure gradients slightly greater than the second ideal marginal value there is a small region of resistive instability beyond which the resistive ballooning mode is stable. In plotting this diagram care must be taken to choose the correct values of θ_0 i.e. those which give rise to the largest unstable regions. Along the second ideal boundary this corresponds to values of $\theta_0 \simeq \pi$, while $\theta_0 \simeq 0$ is found to maximise the resistively unstable zone and is therefore used to plot the $\Delta' = 0$ line.

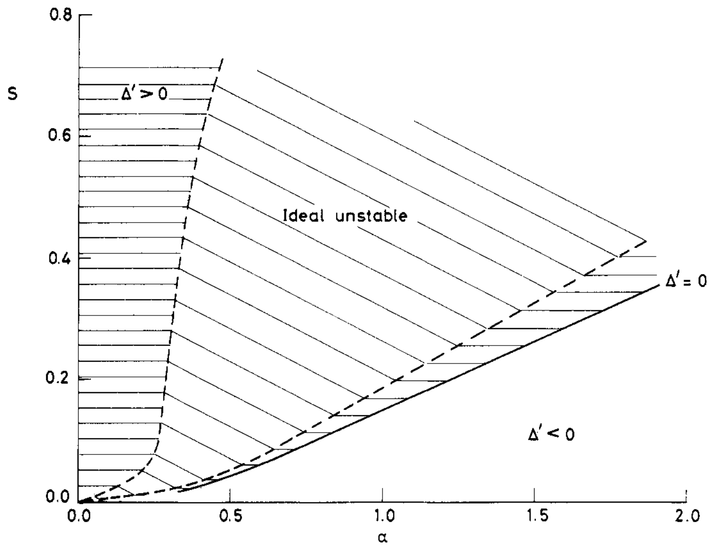

FIG. 3.—The $s - \alpha$ plane showing the $\Delta' = 0$ curve. Note that throughout most of the second region resistive ballooning modes are stable.

These results contrast with those of CORREA-RESTREPO (1985) who found the second region to be mostly unstable to resistive modes. However, Correa-Restrepo considered equilibria constructed in the neighbourhood of the magnetic axis, with q on axis close to unity. He found the resistive interchange mode to be unstable throughout most of the second region, and therefore did not go on to examine resistive ballooning modes. However, when q is substantially larger than one (e.g. in the "confinement region" away from the axis) the resistive interchange mode is very stable and need not be considered further. An evaluation of the expression for Δ' given in CORREA-RESTREPO (1985) shows that indeed $\Delta' > 0$ just beyond the ideally stable region and that Δ' then passes through zero to give a resistive ballooning stable zone. For still large values of α, however, the Δ' of CORREA-RESTREPO (1985) changes sign again by passing through infinity. This does not represent an ideal marginal boundary since it corresponds to $b \to \infty$ in equation (6) rather than $a \to 0$.

5. INCLUSION OF THE SHAFRANOV SHIFT

In the equilibrium corresponding to equation (1) the poloidal component of the magnetic field was taken to be a constant around the flux surface. At high β values it is more realistic to include the modulation of the poloidal field due to the Shafranov shift effect. This is done by writing the poloidal field in the form

$$B_p(\theta) = \frac{B_{p0}}{(1 - \Lambda \cos \theta)} \tag{7}$$

where $\Lambda > 0$. A consistent equilibrium having this poloidal field was constructed by BISHOP and HASTIE (1985) using techniques described in BISHOP (1985). The corresponding ballooning equation and its asymptotic solutions are given in Appendix B.

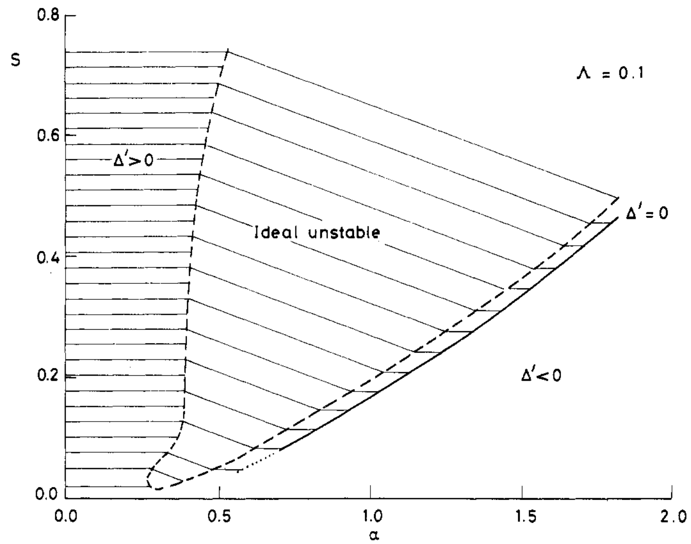

FIG. 4.—The $s - \alpha$ plane showing the stabilising effect of the Shafranov shift on both the ideal marginal stability curves and the $\Delta' = 0$ line. Very little of the second region is now unstable to resistive ballooning modes.

Note that when $\Lambda = 0$ the original s-α model is recovered. Evaluation of Δ' in the second region with $\Lambda = 0.1$ increases the region of stability to resistive ballooning modes. This is shown in the s-α plane in Fig. 4 which also shows the stabilising effect of $\Lambda > 0$ on the ideal stability boundaries. Again a careful study of the effects of varying θ_0 has been made in plotting this diagram, giving $\theta_0 \simeq \pi$ along the second ideal boundary and $\theta_0 = 0$ along the $\Delta' = 0$ curve.

6. CONCLUSIONS

We have shown that while the first ideally stable region is generally unstable to resistive ballooning modes, the second region may be largely stable. If resistive modes do indeed play a role in cross-field transport in the first region then their absence from the second region may be beneficial for Tokamak profiles lying wholly or partly in this region. The relevance of this depends of course on the practical accessibility of the second region. At least five methods of achieving this have been suggested:

(i) Direct profile modification by localised auxiliary heating; the effects of $q_{\text{axis}} > 1$ were discussed theoretically by ANTONSEN *et al.* (1980) and MERCIER (1978), and a computer simulation using these results and showing stable access to the second region was give by SYKES and TURNER (1979).

(ii) Generation of anisotropic pressure, again by auxiliary heating; if the perpendicular pressure can be modulated so as to be larger on the inside of the flux surface then access to the second region becomes possible: FIELDING and HAAS (1978).

(iii) Stabilisation of the ballooning mode by a population of energetic trapped particles: ROSENBLUTH *et al.* (1983); SPONG *et al.* (1985).

(iv) Proximity of a magnetic separatrix as in a divertor Tokamak; this can give direct access to the second region: BISHOP (1986). Indeed the steep pressure gradients observed in the edge region of the H-mode discharge may represent the first experimental observation of second stability.

(v) Shaped plasma cross-sections such as strongly indented beans (CHANCE *et al.*, 1983) may also give access to the second region.

REFERENCES

ANTONSEN T., BASU B., CREW G., ENGLADE R. *et al.* (1980) *Plasma Physics and Controlled Nuclear Fusion Research* (IAEA, Brussels). CN-38/C-3 Vol. 1, p. 83.

BISHOP C. M. and HASTIE R. J. (1985) *Nucl. Fusion* **25** (10), 1443.

BISHOP C. M. (1985) *Construction of Local Axisymmetric MHD Equilibria*, UKAEA, Culham Lab, Abingdon, UK, Rep CLM-R249.

BISHOP C. M. (1986) *Nucl. Fusion* **26** (8), 1063.

CHANCE M. S., DEWAR R. L., FRIEMAN E. A., GLASSER A. H. and GREENE J. M. *et al.* (1979) *Plasma Physics and Controlled Nuclear Fusion Research* (IAEA, Vienna) Vol. I, p. 677.

CHANCE M. S., JARDIN S. C. and STIX T. H. (1983) *Phys. Rev. Lett.* **51** (21), 1963.

CONNOR J. W., HASTIE R. J., MARTIN T. J., SYKES A. and TURNER M. F. (1983) *Plasma Physics and Controlled Nuclear Fusion Research* (IAEA, Baltimore). Vol. III, p. 403.

CONNOR J. W., HASTIE R. J. and MARTIN T. J. (1985) *Plasma Physics* **27**, 1509.

CONNOR J. W., HASTIE R. J. and TAYLOR J. B. (1978) *Phys. Rev. Lett.* **40**, 396.

CONNOR J. W., HASTIE R. J. and TAYLOR J. B. (1979) *Proc. Roy. Soc.* **A365**, 1.

CORREA-RESTREPO D. (1985) *Plasma Phys. Contr. Fusion* **27**, 565.

DRAKE J. F. and ANTONSEN T. M. (1985) *Physics Fluids* **28** (2), 544.

FIELDING P. J. and HAAS F. A. (1978) *Phys. Rev. Lett.* **41**, 801.

FURTH H. P., KILEEN J. and ROSENBLUTH M. N. (1963) *Physics Fluids* **6**, 459.

MERCIER C. (1978) *Plasma Physics and Controlled Nuclear Fusion Research* (IAEA, Innsbruck). Vol. I, p. 701, CN-37/p-3-2.

ROSENBLUTH M. N., TSAI S. T., VAN DAM J. W. and ENGQUIST M. G. (1983) *Phys. Rev. Lett.* **51** (21), 1967.

SPONG D. A., SIGMAR D. J., COOPER W. A. and HASTINGS D. E. (1985) *Physics Fluids* **28** (8), 2494.

STRAUSS H. R. (1981) *Physics Fluids* **24** (11), 2004.

SYKES A. and TURNER M. F. (1979) *Controlled Fusion and Plasma Physics* (EPS, Oxford). Vol. II, p. 161, EP22.

APPENDIX A

Averaging of equation (1) is done by introducing two length scales: an equilibrium length scale θ, and a large scale $u = s\theta$. Averaging over the short scale θ leads to a simplified equation in u:

$$s^2 \frac{\mathrm{d}}{\mathrm{d}u}(1 + u^2)\frac{\mathrm{d}F}{\mathrm{d}u} + \frac{2\,\alpha^2 s}{(1 + u^2)^2}F - \frac{3}{8}\frac{\alpha^4 F}{(1 + u^2)^2} = 0. \tag{A1}$$

The asymptotic solutions to this equation are readily obtained in the form

$$F(u) = a\,F_L + b\,F_S \tag{A2}$$

where

$$F_{S,L} = u^{\lambda}\left[1 + \frac{f_1}{u^2} + \frac{f_2}{u^4} + \dots\right] \tag{A3}$$

$$f_1 = -\lambda/(\lambda - 2) \tag{A4}$$

$$f_2 = \frac{\{(2\alpha^2/s - 3\alpha^4/8s^2) + \lambda(\lambda - 3)\}}{(\lambda - 4)(\lambda - 3)} \tag{A5}$$

where the small solution has $\lambda = -1$ and the large solution has $\lambda = 0$. To calculate Δ' the solution of equation (A1) with initial conditions $F(0) = 1$, $F'(0) = 0$ is matched to the asymptotic form (A2) for large values of u. The values of a and b thereby obtained are used to calculate Δ' from $\Delta' = b/sa$.

APPENDIX B

The ballooning mode equation for $\Lambda \neq 0$ can be written

$$\frac{d}{d\theta}\left\{g(\theta)(1 + G^2)\frac{dF}{d\theta}\right\} + \alpha g(\cos\theta + G\sin\theta)F = 0 \tag{B1}$$

where

$$g(\theta) = 1 - \Lambda\cos\theta \tag{B2}$$

$$g^2\,G(\theta) = s(\theta - \theta_0) + 2\int_0^\theta [g^2]d\theta - \alpha\int_0^\theta [g^3\cos\theta]d\theta + \frac{Q}{\langle g^3\rangle}\int_0^\theta [g^3]d\theta \tag{B3}$$

with

$$Q = s - 2\langle g^2\rangle + \alpha\,\langle g^3\cos\theta\rangle \tag{B4}$$

and the bracket notations are defined by

$$\langle X\rangle = \frac{1}{2\pi}\int X d\theta, \quad [X] = X - \langle X\rangle. \tag{B5}$$

Note that if $\Lambda = 0$ then equation (B1) reduces to equation (1). The asymptotic forms for the solutions of (B1) can be written

$$F(\theta) = \tilde{a}\,F_L + \tilde{b}\,F_S \tag{B6}$$

with

$$F_{S,L} = (s\theta)^{\lambda_{L,S}}\left[1 + \frac{F_1}{s\theta} + \dots\right] \tag{B7}$$

where

$$F_1(\theta) = \sum_{n=1}^{4} f_n\sin(n\theta)$$

$$f_1 = \alpha\left(1 + \frac{9}{4}\Lambda^2\right) - 3\Lambda\left(1 + \frac{\Lambda^2}{4}\right)T \tag{B8}$$

$$f_2 = \frac{3}{4}\Lambda^2\,T - \frac{3}{4}\alpha\Lambda\left(1 + \frac{\Lambda^2}{3}\right) \tag{B9}$$

$$f_3 = -\frac{\Lambda^3}{12}T + \frac{\Lambda^2}{4}\alpha, \quad f_4 = -\frac{\Lambda^3}{32}\alpha \tag{B10}$$

$$T_{L,S} = \frac{\left\{s\lambda_{L,S} + \frac{3}{2}\alpha\Lambda\left(1 + \frac{\Lambda^2}{4}\right)\right\}}{\left(1 + \frac{3}{2}\Lambda^2\right)} \tag{B11}$$

and the indices λ_S and λ_L, corresponding respectively to small and large solutions, satisfy

$$s^2\lambda(\lambda + 1) - \frac{9}{4}\alpha\Lambda^3 = 0. \tag{B12}$$

Again Δ' is calculated from $\Delta' = \tilde{b}/s\tilde{a}$.